

Excellence in Chemistry Research



Announcing our new flagship journal

- Gold Open Access
- Publishing charges waived
- Preprints welcome
- Edited by active scientists



Meet the Editors of ChemistryEurope





Luisa De Cola Università degli Studi di Milano Statale, Italy



Ive Hermans
University of
Wisconsin-Madison, USA



Ken Tanaka Tokyo Institute of Technology, Japan



www.chemcatchem.org



Check for updates

Highly Active and Stable Single Atom Rh₁/CeO₂ Catalyst for CO Oxidation during Redox Cycling

Carlos E. García-Vargas, [a, b] Xavier Isidro Pereira-Hernández, [a] Dong Jiang, [a] Ryan Alcala, [c] Andrew T. DeLaRiva, [c] Abhaya Datye, *[c] and Yong Wang*[a, d]

We report a single atom Rh_1/CeO_2 catalyst prepared by the high temperature ($800\,^{\circ}C$) atom trapping (AT) method which is stable under both oxidative and reductive conditions. Infrared spectroscopic and electron microscopy characterization revealed the presence of exclusively ionic Rh species. These ionic Rh species are stable even under reducing conditions (CO at $300\,^{\circ}C$) due to the strong interaction between Rh and CeO_2 achieved by the AT method, leading to high and reproducible CO oxidation activity regardless of whether the catalyst is reduced or

oxidized. In contrast, ionic Rh species in catalysts synthesized by a conventional impregnation approach (e.g., calcined at 350 °C) can be readily reduced to form Rh nanoclusters/nanoparticles, which are easily oxidized under oxidative conditions, leading to loss of catalytic performance. The single atom Rh_1/CeO_2 catalysts synthesized by the AT method do not exhibit changes during redox cycling hence are promising catalysts for emission control where redox cycling is encountered, and severe oxidation (fuel cut) leads to loss of performance.

Introduction

More stringent environmental regulations have been constantly implemented^[1] with the purpose of mitigating the environmental impact of the consumption of fossil fuels to satisfy societal energy needs.^[2] These ambitious regulations motivated the development of several catalytic technologies for exhaust gas aftertreatment, such as hydrocarbon oxidation catalysts and three-way catalysts (TWC), which have achieved tremendous success for emission abatement.^[3] In view of constant introduction of stringer regulations,^[4] more efficient engines demand the challenging development of catalytic materials exhibiting

excellent low temperature activity, which needs to be maintained regardless the conditions encountered in each technological application, including high temperatures under high engine loads. In real operation conditions, high temperatures can induce sintering of active precious metals into larger particles^[5,6] as well as the oxidative redispersion of small metal nanoparticles into single atoms, both cases resulting in overall loss of CO^[7] and hydrocarbon^[8] oxidation activity. Similarly, expensive precious metals (e.g., Pt, Rh,) that are used in TWC are exposed to high temperatures as well as transient oxidative and reductive environments that result from the engine control system that maintains the air to fuel ratio around the stoichiometric point,[1,3] conditions at which optimal emission abatement by TWC is achieved. The use of fuel cut regimes to improve fuel economy leads to large exotherms under oxidizing conditions, which are particularly harmful to the catalyst. Such harsh redox and thermal conditions damage the structural properties of TWC active phase, hence having a detrimental effect on its activity. [9,10] Therefore, there is an important need to develop materials that perform equally well under reducing as well as oxidizing conditions, helping to comply with the requirements of low temperature activity, high temperature stability, and structural resistance under redox conditions.

The Gene and Linda Voiland School of Chemical Engineering and Bioengineering
Washington State University
99164 Pullman, WA (USA)
E-mail: wang42@wsu.edu
[b] C. E. García-Vargas
Environmental Molecular Sciences Laboratory,

[a] C. E. García-Vargas, Dr. X. I. Pereira-Hernández, Dr. D. Jiang, Dr. Y. Wang

Environmental Molecular Sciences Laboratory, Pacific Northwest National Laboratory 99354 Richland, WA (USA) [c] R. Alcala, Dr. A. T. DeLaRiva, Dr. A. Datye

[c] R. Alcala, Dr. A. T. DeLaRiva, Dr. A. Datye Department of Chemical and Biological Engineering and Center for Microengineered Materials University of New Mexico 87131 Albuquerque, NM (USA) E-mail: datye@unm.edu

[d] Dr. Y. Wang Institute for Integrated Catalysis aPacific Northwest National Laboratory 99354 Richland, WA (USA)

Supporting information for this article is available on the WWW under https://doi.org/10.1002/cctc.202201210

This publication is part of a Special Collection on "Developments in Surface Organometallic and Heterogeneous Single-Atom Catalysts". Please check the ChemCatChem homepage for more articles in the collection.

© 2023 The Authors. ChemCatChem published by Wiley-VCH GmbH. This is an open access article under the terms of the Creative Commons Attribution License, which permits use, distribution and reproduction in any medium, provided the original work is properly cited.

tion for their application in emissions abatement, catalyzing reactions such as NO $_{\rm x}$ reduction, $^{[11-13]}$ N $_{\rm 2}$ O decomposition $^{[14-16]}$ and CO oxidation. $^{[17-24]}$ On the latter, early kinetic studies by Zafiris $^{[17]}$ and Bunluesin $^{[18]}$ et al. on model Rh/CeO $_{\rm 2}$ catalysts revealed a Langmuir-Hinshelwood reaction mechanism, in which CO and O $_{\rm 2}$ compete for the metallic Rh active sites. Later studies focused on the effect of synthesis method on the structural and catalytic properties of Rh/CeO $_{\rm 2}$ systems, which observed complex surface and subsurface Rh species $^{[25]}$ and suggested that highly dispersed $^{[26]}$ and oxidic $^{[21]}$ Rh nanoparticles $^{[27]}$ were very active for CO oxidation. Such findings have recently motivated studies about the effect of highly

Ceria-supported Rh materials have caught increasing atten-

3, 1, Downloaded from https://chemisty-europe.conlinelibrary.wiely.com/doi/10.1002/cctc.20201210 by Purdue University (West Lafayette), Wiley Online Library on [14/12/2023]. See the Terms and Conditions (https://onlinelibrary.wiely.com/rems-and-conditions) on Wiley Online Library for rules of use; OA articles are governed by the applicable Creative Commons Licensea

Research Article
doi.org/10.1002/cctc.202201210

Research Publishing

European Chemical
Societies Publishing

dispersed Rh species on their activity for CO oxidation. Derevyannikova^[23] et al. prepared a Rh-doped CeO₂ material using co-precipitation method and concluded that such type of Rh_xCe_{1-x}O₂ solid solutions, in addition to having high amounts of unused Rh species in the bulk, are prone to large RhO_x surface aggregation accompanied with loss of CO oxidation activity as a consequence of their poor thermal stability. Jeong^[28] et al. obtained highly dispersed RhO_x ensembles of ~0.9 nm size on CeO₂ via hydrothermal treatment, showing notable CO and hydrocarbon oxidation but at the expense of relatively high Rh loadings (~2 wt.%). Hüsley[29] et al. successfully designed a heteropoly acid-supported Rh single atom catalyst which was highly active for CO Oxidation, but with limited thermal stability. Han et al. prepared TiO₂- & CeO₂supported Rh single atom catalysts using ultra-low Rh loading with adsorption and co-precipitation methods, respectively. The TiO₂-supported Rh showed stable time on stream performance but poor low temperature activity ($T_{90} > 190$ °C), while nuclearity of Rh species was not clear upon H2 activation and thermal treatments. [30] The CeO₂-supported Rh, made by co-precipitation method, showed significant deactivation over time, but better low temperature activity ($T_{90} \sim 145\,^{\circ}\text{C}$) than the TiO_2 -supported Rh. However, the links between deactivation and Rh nuclearity upon initial H₂ activation remain to be clarified. [31] Most recently, Vera et al. stabilized low loadings of Rh (< 0.4 wt.%) on Zr_{0.15}Ce_{0.85}O₂ mostly as atomically dispersed species with good low temperature CO oxidation performance, but its thermally stability was not studied.[32] Evidently, despite the described research efforts, the development of Rh-based materials capable of simultaneously exhibiting robust thermal stability, intrinsic low temperature activity and structural resistance under redox environments remains elusive.

Results and Discussion

In this work, thermally stable single atom Rh₁/CeO₂ catalysts were synthesized using a high temperature atom trapping (AT) method (800°C calcination in air for 1 hour) we recently reported.^[7,33-35] In such catalysts, denoted as 0.6 wt.% Rh/ CeO₂(AT), the presence of Rh prevents the sintering of CeO₂, leading to a surface area of 39 m²/g as opposed to 18 m²/g for the CeO₂(AT) support which was treated under the same AT synthesis conditions (Table S1). We have previously reported that the trapping mechanism of Rh atoms on CeO₂ likely involves Rh surface diffusion[36-40] instead of RhO_x mobility by volatilization, as is the case for PtO₂ trapping on CeO₂.^[7] The CO oxidation performance of the 0.6 wt.% Rh/CeO₂(AT) catalyst was compared with that of a catalyst synthesized with a conventional approach (e.g., calcination at 350 °C) which is denoted as 0.6 wt.% Rh/CeO₂(350). As shown in Figure 1, 0.6 wt.% Rh/ CeO₂(AT) is more reactive than 0.6 wt.% Rh/CeO₂(350), which is reflected by the temperatures to reach 50% CO conversion (T₅₀) of 129 and 160°C, respectively, and achieve 90 % CO conversion (T_{90}) at < 150 °C (The 150°C Challenge by DOE^[4]). A reductive treatment (5 %CO at 275 °C for 30 minutes) did not affect the light-off behavior of the 0.6 wt.% Rh/CeO₂(AT)-Red catalyst, but

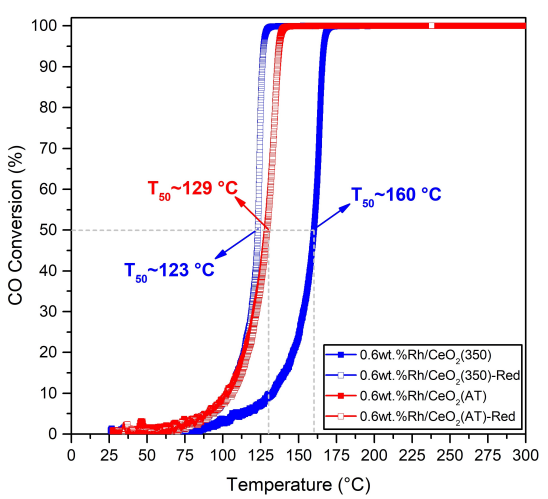


Figure 1. CO oxidation light-off curves for 0.6 wt.% RhCeO₂(AT) & 0.6 wt.% RhCeO₂(350) catalysts before and after reduction. Reaction conditions: 1% CO, $4\%O_2$ balanced Ar. 20 mg of catalyst diluted with 500 mg SiC. WHSV = 300,000 mL/gcat·min.

on the other hand shifted T₅₀ by approximately 37 °C (from 160 to 123°C) for the 0.6 wt.% Rh/CeO₂(350)-Red catalyst. Apparently, 0.6 wt.% Rh/CeO₂(AT) catalyst not only exhibits the stable light-off behavior with and without the reductive treatment, but also shows a similar activity as the reduced 0.6 wt.% Rh/ $CeO_2(350)$ -Red catalyst (e.g., T_{50} of 129 vs 123°C, respectively). This suggests that the nature of active sites in the 0.6 wt.% Rh/ CeO₂(AT) catalyst is different from that in the 0.6 wt.% Rh/ CeO₂(350) catalyst and remains the same under reductive conditions. This is further supported by the fact that the reaction orders with respect to CO and O2 partial pressures remain the same, $\sim 0.26 \pm 0.02$ and 0.02 ± 0.01 respectively, for the 0.6 wt.% Rh/CeO₂(AT) catalyst with and without reductive treatment (Figure S1), whereas those reaction orders with respect to CO and O₂ for metallic Rh/CeO₂ samples are expected to be ~ -1 and $\sim +1$, as has been extensively reported in previous literature. [17,20,41] The Arrhenius plot of the 0.6 wt.% Rh/ CeO₂(AT) catalyst along with a comparisson of the experimentally determined activation energy against other Rh-supported catalysts for CO oxidation are reported in Figure S2 and Table S2.

To further understand the nature of both $0.6 \text{ wt.}\% \text{ Rh/CeO}_2(\text{AT})$ and $0.6 \text{ wt.}\% \text{ Rh/CeO}_2(350)$ catalysts with and without reductive treatment, in situ CO-Diffuse Reflectance Infrared Fourier Transform Spectroscopy (DRIFTS) studies were conducted. As shown in Figure 2a, four main infrared bands of maximum intensity at frequencies of 2121 cm^{-1} , 2106 cm^{-1} , 2082 cm^{-1} and 2016 cm^{-1} are clearly observed on the assynthesized $0.6 \text{ wt.}\% \text{ Rh/CeO}_2(\text{AT})$ catalyst spectra after 15 minutes under CO oxidation at $125 \,^{\circ}\text{C}$. The two peaks of lowest frequency are assigned as the symmetric ($2082 \, \text{cm}^{-1}$) and asymmetric ($2016 \, \text{cm}^{-1}$) vibrations of Rh gem-dicarbonyl species ($2016 \, \text{cm}^{-1}$) which Rh is present as cationic with oxidation state of $2016 \, \text{cm}^{-1}$ are typically assigned to linearly adsorbed Rh carbonyl species

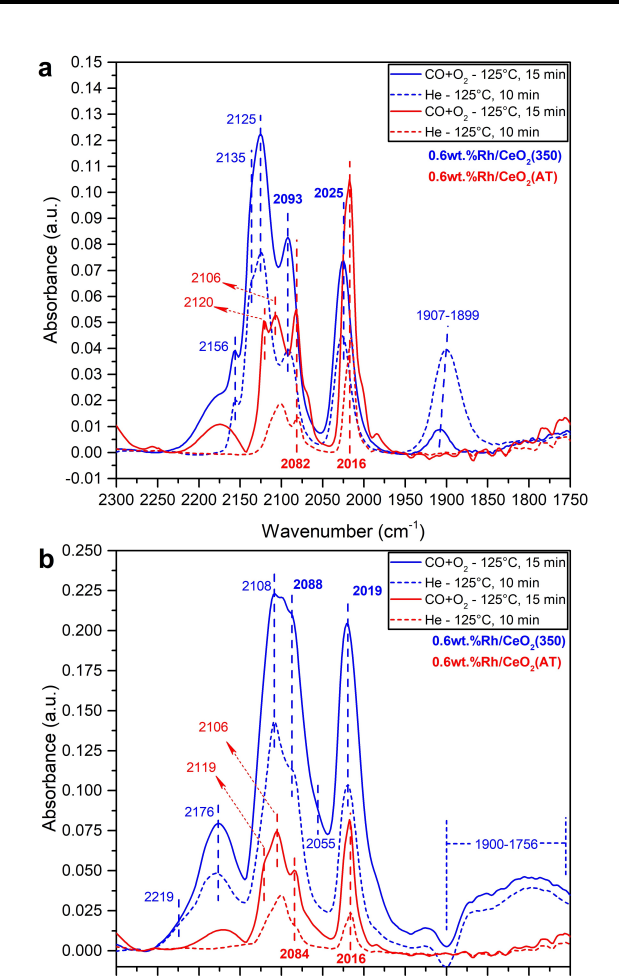


Figure 2. In situ CO oxidation (1 %CO, $4 \%O_2$) & He desorption DRIFTS before and after reduction (5 %CO 275 °C for 30 minutes) for a) 0.6 wt.% Rh/CeO₂(AT) and b) 0.6 wt.% Rh/CeO₂(350). Reduced samples are denoted by addition of -Red to the as-synthesized name.

2300 2250 2200 2150 2100 2050 2000 1950 1900 1850 1800 1750

Wavenumber (cm⁻¹)

where Rh is present as cationic with oxidation state > 1+, i.e., Rh³⁺—CO and Rh²⁺—CO, respectively. [43-45] Desorption in He leads to reduced intensities of all four peaks except that carbonyls desorb easier on Rh³⁺–CO (2121 cm⁻¹) than Rh²⁺–CO species (2106 cm⁻¹).^[45] Minor or negligible frequency redshifts of the symmetric (2082 cm⁻¹) and asymmetric (2016 cm⁻¹) vibrations of Rh gem-dicarbonyl species (Rh⁺–(CO)₂), attributed to dipole-dipole coupling, $^{\left[46-48\right] }$ are characteristic of such ionic metal carbonyls upon desorption.^[42,49,50] The absence of such changes in the spectrum taken after desorption with He for 10 minutes further confirms the Rh⁺(CO)₂ assignment. Overall, the detection of exclusively ionic Rh carbonyl species on 0.6 wt.% Rh/CeO₂(AT) catalyst strongly suggests that Rh is atomically dispersed.^[51] It is important to note that the same ionic Rh species, and very similar IR peak intensities, are present in the spectra taken for the 0.6 wt.% Rh/CeO₂(AT)-Red catalyst even after 15 minutes of CO oxidation and after 10 minutes of desorption with Helium, as seen in Figure 2a. This again confirms that the nature of Rh species remains the same after reductive treatment and is consistent with the unchanged CO oxidation activity with and without reductive treatment for the 0.6 wt.% Rh/CeO₂(AT) catalyst shown in Figure 1.

As shown in Figure 2b, the spectrum of 0.6 wt.% Rh/ CeO₂(350) catalyst under CO oxidation also present four peaks characteristic of Rh gem-dicarbonyl doublet (2089 cm⁻¹ & 2018 cm⁻¹) and Rhⁿ⁺—CO species (2110 cm⁻¹ & 2103 cm⁻¹). Notably, the well-defined peak at 2121 cm⁻¹ observed in spectra of 0.6 wt.% Rh/CeO₂(AT) catalyst appears significantly less intense. The same ionic Rh species seem to be observed upon desorption of CO with He. Given the presence of exclusively ionic rhodium carbonyl species in the IR spectra of 0.6 wt.% Rh/CeO₂(350) catalyst, it can be inferred that Rh is also atomically dispersed on such catalyst. On the other hand, in addition to the four peaks representing ionic Rh species, the spectrum of 0.6 wt.% Rh/CeO₂(350)-Red shows narrow & broad features at 2056 cm⁻¹ and 1926–1756 cm⁻¹ respectively. These features are widely accepted to represent linearly adsorbed (Rh_x-CO) and bridged (Rh_x-CO-Rh_x) carbonyls on metallic Rh, respectively. [42,45,50-54] An easier CO desorption from Rhx rather than ion ionic Rh species is observed upon exposure to He. Such observation suggests a weaker interaction of CO with the Rh_x species, which seems to be correlated with the improved activity observed in Figure 1. Since the presence of peaks at 2156 cm⁻¹, 2219 cm⁻¹ & 2176 cm⁻¹ (Rh-NCO) and 1907– 1889 cm⁻¹ (Rh-nitrosyl) indicates that residual nitrates remain from static air calcination at 350 °C, flowing air calcination at 350 for ~24 h (sample denoted as 0.6 wt.% Rh/CeO₂(350-F/Air-24 h)) was used to determine if the extent of nitrates content significantly changes the DRIFTS spectra and light-off curves before and after reduction. From Figures S3a&b, it can be noticed that all the IR peaks were slightly red-shifted (by ~5-7 cm⁻¹) compared to the DRIFTS spectra of 0.6 wt.% Rh/ CeO₂(350), which indicates better removal of nitrates. Similarly, the complete disappearance of all the peaks corresponding to rhodium isocyanates (Rh-NCO) at 2156 cm⁻¹ in Figure 2a and 2219 cm⁻¹ & 2176 cm⁻¹ in Figure 2b, demonstrates superior nitrates removal upon calcination in flowing air. Although some Rh-nitrosyl species at 1882–1876 cm⁻¹ (Figure S3a) remain (but rather less intense) on 0.6 wt.% Rh/CeO₂(350-F/Air-24 h), it can be observed that its light-off behavior (Figure S4) is still affected upon changes in redox environments. Therefore, it can be concluded that the extent of nitrates content is not the key factor that allows Rh/CeO₂ catalyst to maintain a stable light-off behavior under variable redox atmospheres, as it is the case for the 0.6 wt.% Rh/CeO₂(AT) sample.

Despite the existence of exclusively ionic Rh species in both as-synthesized 0.6 wt.% Rh/CeO₂(AT) and 0.6 wt.% Rh/CeO₂ samples (confirmed by the presented DRIFTS results), their differences in reactivity observed in Figure 1 might suggest a different nature of such ionic species. However, since significant differences in the CO adsorption strength among both catalysts do not appear to exist upon desorption with He (Figures 2a and 2b), we decided to further investigate their redox properties using CO-TPR experiments. As shown in Figure 3a for the assynthesized samples, despite both having similar onset temperatures, 0.6 wt.% Rh/CeO₂(AT) is the catalyst that exhibits the first



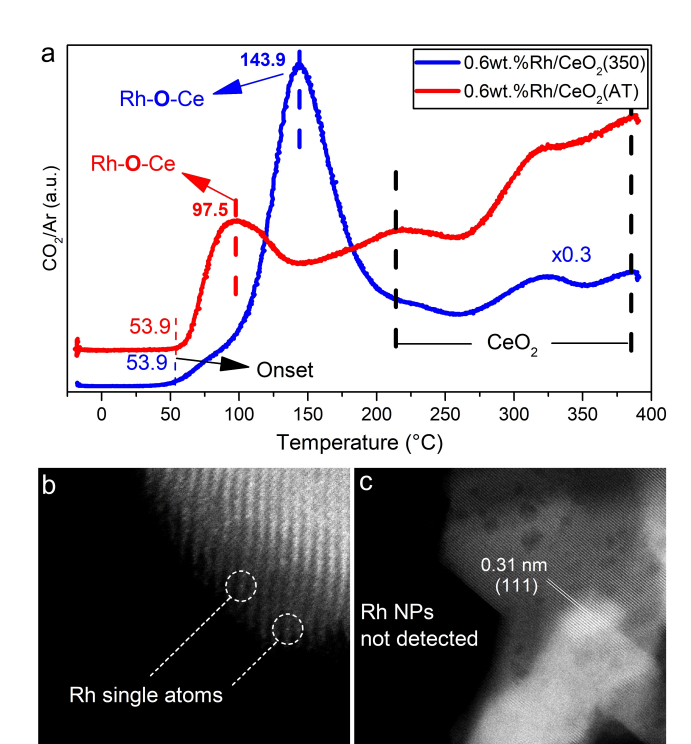


Figure 3. a) CO-TPR profiles of 0.6 wt.% Rh/CeO₂(AT) & 0.6 wt.% Rh/ CeO₂(350). STEM images of 0.6 wt.% Rh/CeO₂(AT)-Red using b) LAADF and c) HAADF detectors.

reduction peak at the lowest temperature (97.5 °C compared to 143.9°C for 0.6 wt.% Rh/CeO₂(350)), which correlates with its superior light-off performance. The consumed O* estimated from the CO-TPR (T < 200 $^{\circ}$ C) is 5079 and 833 umolO* for 0.6 wt.% Rh/CeO₂(350) and 0.6 wt.% Rh/CeO₂(800) respectively (Figure S5 and Table S3). It is noteworthy that despite the AT sample having ~6 times less O* available than the low temperature calcined catalyst, it still exhibits better low temperature activity, which further suggests a distinct nature of Rh–CeO₂ interaction that stems from AT synthesis and favors CO oxidation at lower temperatures, similar to what we reported for Pt/CeO₂^[34] and Cu/CeO₂^[38] prepared by AT.

Consistently, the unchanged light-off performance and DRIFTS spectra for 0.6 wt.% Rh/CeO₂(AT), before and after reduction provides further evidence of the unique Rh–CeO₂ interaction that results from the AT method. In addition, the Rh nuclearity was investigated by STEM imaging. Despite the poor Z-contrast between Rh and Ce, which difficult the observation of Rh single atoms, [55,56] Figure 3b shows Rh₁ atoms located in the thinnest regions oriented off the zone axis for the 0.6 wt.% Rh/CeO₂(AT) catalyst. On the other hand, Rh nanoparticles/ clusters, which can be readily detected due to higher contrast with Ce, were not observed in the Figure 3c STEM image of 0.6 wt.% Rh/CeO₂(AT)-Red, in agreement with our DRIFTS analysis. In contrast, only (111) planes of CeO₂ were observed even for the brightest features seen in Figure 3c (see additional images in Figure S6).

To further explore structural changes on 0.6 wt.% Rh/ CeO₂(AT) and 0.6 wt.% Rh/CeO₂(350) catalysts under stronger reductive conditions, both samples were studied using in situ DRIFTS. After exposure to 5% CO at 300°C for 60 minutes followed by cooling down to 125°C, DRIFTS spectra were collected. The reduced samples at 300°C were denoted as 0.6wt.% Rh/CeO₂(AT)-Red300 and 0.6 wt.% Rh/CeO₂(350)-Red300 respectively. As shown in Figure 4, the collected spectrum of the former reveals the presence of exclusively Rh⁺ (CO)₂ species, which vibrations are represented by the peaks at 2086 cm⁻¹ & 2027 cm⁻¹, whereas the latter, in addition to the same Rh+(CO)₂ species, displays the presence of linearly adsorbed (Rh_x-CO) and bridged (Rh_x-CO-Rh_x) carbonyls on Rh_x species represented by the peaks at 2056 cm⁻¹ and 1926-1753 cm⁻¹. The presence of exclusively ionic Rh species (i.e., Rh¹⁺(CO)₂) in the spectra for 0.6 wt.% Rh/CeO₂(AT)-Red300 reveals the tremendous stability of cationic Rh species obtained by AT synthesis method, even under such harsh environment. On the other hand, partial reduction of ionic Rh to Rh_x-like species is readily observed in the spectrum of 0.6 wt.% Rh/ CeO₂(350)-Red300.

It is worth noting that the stability of the ionic Rh species in 0.6 wt.% Rh/CeO₂(AT)-Red300 against reduction seems to be an intrinsic characteristic derived from the AT method of synthesis rather than a consequence of the well-known CO-assisted Rh_x crystallite disruption effect. [57-59] Such Rhx redispersion has been reported to occur for Rh-supported particles heat-treated below ~200°C under CO atmospheres, while our samples have been subjected up to 300 °C under CO for 1 hour. On the other hand, the presence of bridged- and linearly-adsorbed carbonyl species in the spectra of 0.6 wt.% Rh/CeO₂(350)-Red300 of Figure 4, suggests the formation of rhodium species which might be bigger than the reported threshold size^[57,60-63] for redispersion.

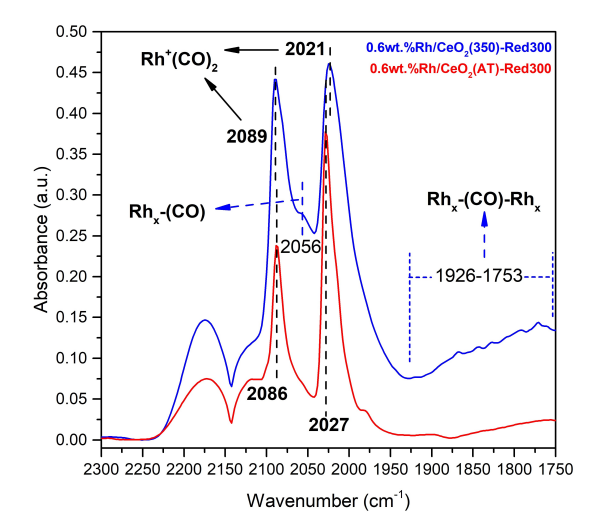


Figure 4. DRIFTS spectra of 0.6 wt % Rh/CeO₂(AT) and 0.6 wt % Rh/CeO₂(350) after reduction in 5 %CO at 300 °C and measured at 125 °C.



Conclusion

Here, Rh₁/CeO₂ catalysts prepared by the AT method are thermally stable up to 800 °C in oxidative environments, while at the same time exhibiting excellent low temperature CO oxidation activity, as seen by low temperature CO-TPR peaks and reproducible light-off curves, thus overcoming the challenge of sintering under elevated temperatures and oxidative/reductive cycling environments. With the use of *in situ* DRIFTS measurements and STEM imaging, a unique type of ionic Rh species was revealed, which are capable of withstanding high temperature and redox environments and has tremendous potential for their application under real TWC conditions.^[64]

Experimental Section

Catalyst Synthesis: Polyhedral CeO₂ was prepared by thermal decomposition of Cerium(III) nitrate hexahydrate Ce(NO)₃·6H₂O 99.999% purity from Sigma-Aldrich) in air at 350°C for 1 hour, and was named as CeO₂(350). The grain size was maintained smaller than 0.149 mm with the use of 100-mesh number sieve. The solutions for incipient wetness impregnation of the CeO₂(350) support were prepared with Rhodium(III) nitrate hydrate Rh- $(NO_3)_3 \cdot xH_2O \sim 36\%$ Rh from Sigma) and deionized water. A loading of ~0.6 wt.% (equivalent to 1 mol.%) was targeted. After impregnation, the samples were dried in air at 150 °C for 1 hour. The dried product was then sieved with a 100-mesh number sieve. Calcination at 350 °C was done in flowing air for 6 hours, while calcination at atom trapping conditions (800°C for 1 h) was carried in static air using a furnace. The heating rate used in both cases was 10 °C/min and the nomenclature given were 0.6 wt.% $Rh/CeO_2(350)$ and 0.6 wt.% Rh/CeO₂(AT) respectively. The CeO₂(350) samples that were treated under atom trapping conditions were denoted as

Surface Area Measurements: Nitrogen sorption experiments were conducted on a Micromeritics TriStar II 3020 physisorption analyzer at $-196\,^{\circ}\text{C}$ using ultra-high purity $N_2.$ The specific surface areas of the catalysts were calculated based on the Brunauer-Emmett-Teller (BET) model. Catalysts were degassed at 150 $^{\circ}\text{C}$ for 1 h under vacuum before measurements were taken.

CO Oxidation: The CO oxidation reaction was conducted in an atmospheric pressure fixed bed flow reactor system using an Agilent 3000 Micro Gas Chromatograph equipped with a mol sieve and TCD detector. The catalyst was loaded into a 4.0-mm-i.d× 40.64-cm-long quartz tube packed in between inert quartz wool. The catalyst bed temperature was controlled with PID temperature controller, and a thermocouple placed inside the quartz tube. The light-off curves were carried out using 20 mg of Catalyst and 500 mg of inert SiC, a heating rate of 2 or 3 °C/min and a GHSV of 300,000 h⁻¹ and gas concentrations of 1%CO, 4%O₂ balanced Argon. Reductive treatments were done at 275 °C with 75 mL/min of 5%CO/Ar for 30 minutes. Under the same conditions the samples were cooled down to room temperature for a subsequent light-off curve. Kinetic measurements were carried out at $X_{co} < 10$ %.

DRIFTS: DRIFTS spectra were acquired with a Tensor 27 from Bruker, coupled with a Praying Mantis[™] Diffuse Reflection Accessory from Harrick. Approximately 50–60 mg of sample were used for each experiment. An initial pre-treatment was done by heating the sample from 30–125 °C while flowing 50 mL/min of UHP He to remove moisture. Once at 125 °C the sample was treated for 30 minutes, and the background was acquired. Spectra taken

during CO oxidation was collected for 15 minutes, starting immediately after the sample was exposed to 6 mL/min of 10 %CO/He, 30 mL/min of He and 24 mL/min of 10 %O₂/He. After CO oxidation measurements, desorption spectra were acquired for 10 minutes while 15 mL/min of UHP He followed by the same flow of 10 %O₂/ He were used. Reduction treatments were done by initially heating the sample from 125 °C to 275 °C while flowing 15 mL/min of UHP He. At 275 °C, 30 minutes of reduction with 30 mL/min of 10 %CO/ He followed by 30 minutes of desorption with 15 mL/min UHP of He was carried out. Collection of spectra during CO oxidation, He desorption and O2 flow for the reduced sample was done after cooling from 275 °C to 125 °C using 15/min of UHP He. Temperature-programmed CO-reduction DRIFTS spectra was collected by loading 50-60 mg of fresh 0.6 wt.% Rh/CeO₂(350) and 0.6 wt.% Rh/ CeO₂(AT) sample. Background was taken at 30 °C while 50 mL/min were flowing. Subsequently, 15 mL/min of 10 %CO/He were flowed, and spectra were taken every 10 °C while temperature was increased from 30-300 °C. At 300 °C spectra were taken for 1 hour and during the cooling ramp from 300-125 °C every 10 °C. Once 125°C temperature was reached, spectra were taken for 60 minutes.

CO-TPR: CO-TPR measurements were done with an Autochem 2920 from Micromeretics. The analysis of products was conducted with a Thermostar GSD 320 T Quadrupole Mass Spectrometer (QMS) from Pfeiffer Vaccum, equipped with a Secundary Electron Multiplier (SEM). Approximately 100 mg of sample, a total flow rate of 100 sccm/min and temperature ramps of $10\,^{\circ}\text{C/min}$ were used in all cases. An oxidative pre-treatment was done using $10\,^{\circ}\text{C}_2$ /He while heating from room temperature to $400\,^{\circ}\text{C}$ and held for 60 minutes. Then the temperature was decreased to $-20\,^{\circ}\text{C}$ and the flow was changed to UHP Helium and maintained for 60 minutes until the QMS mass-to-charge rations were stable. The temperature-programmed reduction was performed using $10\,^{\circ}\text{CO/He}$ from -20 to $400\,^{\circ}\text{C}$.

Acknowledgements

This work is primarily supported by DOE/BES Catalysis Science program, grant DE-FG02-05ER15712. C. E. G.-V. thanks Fulbright Colombia and Colciencias for the financial support provided to pursue a Ph.D. This work made use of instruments in the Electron Microscopy Core of the Univ. of Illinois Chicago RRC.

Conflict of Interest

The authors declare no conflict of interest.

Data Availability Statement

The data that support the findings of this study are available in the supplementary material of this article.

Keywords: Rh single atom \cdot Rh/CeO $_2$ \cdot CO Oxidation \cdot REDOX cycling \cdot TWC

- [1] M. V. Twigg, Catal. Today 2011, 163, 33-41.
- [2] A. Wang, L. Olsson, *Nat. Catal.* **2019**, *2*, 566–570.

- [3] P. Granger, V. I. Parvulescu, Chem. Rev. 2011, 111, 3155-3207.
- [4] U. S. D. R. I. V.E, "Advanced Combustion and Emission Control Technical Team Roadmap," can be found under https://www1.eere.energy.gov/vehiclesandfuels/pdfs/program/acec_roadmap_june2013.pdf, 2013.
- [5] T. R. Johns, R. S. Goeke, V. Ashbacher, P. C. Thüne, J. W. Niemantsverdriet, B. Kiefer, C. H. Kim, M. P. Balogh, A. K. Datye, J. Catal. 2015, 328, 151–164.
- [6] H. Xiong, E. Peterson, G. Qi, A. K. Datye, Catal. Today 2016, 272, 80-86.
- [7] J. Jones, H. Xiong, A. T. DeLaRiva, E. J. Peterson, H. Pham, S. R. Challa, G. Qi, S. Oh, M. H. Wiebenga, X. I. Pereira Hernández, Y. Wang, A. K. Datye, Science 2016, 353, 150–154.
- [8] E. D. Goodman, A. C. Johnston-Peck, E. M. Dietze, C. J. Wrasman, A. S. Hoffman, F. Abild-Pedersen, S. R. Bare, P. N. Plessow, M. Cargnello, *Nat. Catal.* 2019, 2, 748–755.
- [9] A. Fathali, F. Wallin, A. Kristoffersson, M. Laurell, in SAE Tech. Pap., SAE International, 2015.
- [10] J. C. Summers, L. L. Hegedus, Ind. Eng. Chem. Prod. Res. Dev. 1979, 18, 318–324.
- [11] A. Bueno-López, I. Such-Basáñez, C. Salinas-Martínez De Lecea, J. Catal. 2006, 244, 102–112.
- [12] M. Adamowska, A. K. Krztoná, M. Najbar, J. Zef Camra, G. Rald Djé Ga-Mariadassou, P. Da Costa, Appl. Catal. B 2009, 90, 535–544.
- [13] J. Ohyama, T. Nishiyama, A. Satsuma, ChemCatChem 2018, 10, 1651– 1656.
- [14] V. Rico-Pérez, A. Bueno-López, Appl. Sci. 2014, 4, 468–481.
- [15] H. Zhu, Y. Li, X. Zheng, Appl. Catal. A 2019, 571, 89–85.
- [16] S. Parres Esclapez, N₂O Decomposition Rhodium/Ceria Catalysts: From Principles to Practical Application, University of Alicante, 2011.
- [17] G. S. Zafiris, R. J. Gorte, J. Catal. 1993, 143, 86-91.
- [18] T. Bunluesin, H. Cordatos, R. Gorte, J. Catal. 1995, 157, 222-226.
- [19] H. Cordatos, T. Bunluesin, J. Stubenrauch, J. M. Vohs, R. J. Gorte, J. Phys. Chem. 1996, 100, 785–789.
- [20] I. Manuel, C. Thomas, C. Bourgeois, H. Colas, N. Matthess, G. Djéga-Mariadassou, Comparison between Turnover Rates of CO Oxidation over Rh0 or Rhx + Supported on Model Three-Way Catalysts. 2001.
- [21] D. A. J. M. Ligthart, R. A. Van Santen, E. J. M. Hensen, Angew. Chem. Int. Ed. 2011, 50, 5306–5310; Angew. Chem. 2011, 123, 5418–5422.
- [22] K. Klára klára ševčíková, T. Kolářová, T. Skála, N. Tsud, M. Václavů, V. Václavů, Y. Lykhach, V. Matolín, V. Nehasil, Appl. Surf. Sci. 2015, 332, 747–755.
- [23] E. A. Derevyannikova, T. Y. Kardash, L. S. Kibis, E. M. Slavinskaya, V. A. Svetlichnyi, O. A. Stonkus, A. S. Ivanova, A. I. Boronin, *Phys. Chem. Chem. Phys.* 2017, 19, 31883–31897.
- [24] L. S. Kibis, T. Y. Kardash, E. A. Derevyannikova, O. A. Stonkus, E. M. Slavinskaya, V. A. Svetlichnyi, A. I. Boronin, J. Phys. Chem. C 2017, 121, 26925–26938.
- [25] S. Imamura, T. Yamashita, R. Hamada, Y. Saito, Y. Nakao, N. Tsuda, C. Kaito, J. Mol. Catal. A 1998, 129, 249–256.
- [26] V. Rico-Pérez, M. Ángeles Velasco Beltrán, Q. He, Q. Wang, C. Salinas Martínez de Lecea, A. Bueno López, Catal. Commun. 2013, 33, 47–50.
- [27] G. Munuera, A. Fernandez, A. R. Gonzalez-Elipe, Stud. Surf. Sci. Catal. 1991, 71, 207–219.
- [28] H. Jeong, G. Lee, B.-S. Kim, J. Bae, J. Woo Han, H. Lee, S. Korea, J. Am. Chem. Soc. 2018, 140, 9558–9565.
- [29] M. J. Hülsey, B. Zhang, Z. Ma, H. Asakura, D. A. Do, W. Chen, T. Tanaka, P. Zhang, Z. Wu, N. Yan, Nat. Commun. 2019, 10, 1330.
- [30] B. Han, R. Lang, H. Tang, J. Xu, X. K. Gu, B. Qiao, J. Liu, Chin. J. Catal. 2019, 40, 1847–1853.
- [31] B. Han, T. Li, J. Zhang, C. Zeng, H. Matsumoto, Y. Su, B. Qiao, T. Zhang, Chem. Commun. 2020, 56, 4870–4873.
- [32] L. H. Vieira, J. M. Assaf, E. M. Assaf, Mater. Lett. 2020, 277, 128354.
- [33] D. Kunwar, S. Zhou, A. De La Riva, E. Peterson, H. Xiong, X. I. Pereira Hernandez, S. C. Purdy, R. Ter Veen, H. H. Brongersma, J. T. Miller,

- H. Hashiguchi, L. Kovarik, S. Lin, H. Guo, Y. Wang, A. Datye, *ACS Catal.* **2019**, *9*, 3978–3990.
- [34] X. I. Pereira-Hernández, A. DeLaRiva, V. Muravev, D. Kunwar, H. Xiong, B. Sudduth, M. Engelhard, L. Kovarik, E. J. M. Hensen, Y. Wang, A. K. Datye, Nat. Commun. 2019, 10, 1358.
- [35] R. Alcala, A. DeLaRiva, E. J. Peterson, A. Benavidez, C. E. Garcia-Vargas, D. Jiang, X. I. Pereira-Hernández, H. H. Brongersma, R. Ter Veen, J. Staněk, J. T. Miller, Y. Wang, A. Datye, Appl. Catal. B 2021, 284, 119722.
- [36] G. L. Kellogg, N. C. Bartelt, Surf. Sci. 2005, 151–157.
- [37] G. L. Kellogg, Phys. Rev. Lett. 1994, 72.
- [38] C. E. García-Vargas, G. Collinge, D. Yun, M.-S. Lee, V. Muravev, Y.-Q. Su, X. I. Pereira-Hernández, D. Jiang, V.-A. Glezakou, E. J. M. Hensen, R. Rousseau, A. K. Datye, Y. Wang, ACS Catal. 2022, 12, 13649–13662.
- [39] M. lachella, T. Le Bahers, D. Loffreda, J. Phys. Chem. C 2018, 122, 3824–3837.
- [40] Q. Wan, F. Wei, Y. Wang, F. Wang, L. Zhou, S. Lin, D. Xie, H. Guo, Nanoscale 2018, 10, 17893–17901.
- [41] T. Bunluesin, H. Cordatos, R. J. Gorte, J. Catal. 1995, 157, 222-226.
- [42] A. C. Yang, C. W. Garland, A. C. Yang, J. Phys. Chem. 1957, 61, 1504– 1512.
- [43] A. K. Smith, F. Hugues, A. Theolier, J. M. Basset, R. Ugo, G. M. Zanderighi, J. L. Bilhou, V. Bilhou-Bougnol, W. F. Graydon, *Inorg. Chem.* 1979, 18, 3104–3112.
- [44] J. P. Wey, W. C. Neely, S. D. Worley, J. Catal. 1992, 134, 378–381.
- [45] S. Trautmann, M. Baerns, J. Catal. 1994, 150, 335–344.
- [46] G. Blyholder, J. Phys. Chem. 1964, 68, 2772–2777.
- [47] R. M. Hammaker, S. A. Francis, R. P. Eischens, Infrared Study of Intermolecular Interactions for Carbon Monoxide Chemisorbed on Platinum, Pergamon Preen Ltd, 1965.
- [48] A. Crossley, D. A. King, Surf. Sci. 1977, 68, 528–538.
- [49] J. T. Yates, T. M. Duncan, R. W. Vaughan, J. Chem. Phys. 1979, 71, 3908–3915.
- [50] J. T. Yates, T. M. Duncan, S. D. Worley, R. W. Vaughan, J. Chem. Phys. 1979, 70(03), 1219–1224, DOI 10.1063/1.437603.
- [51] R. R. Cavanagh, J. T. Yates, J. Chem. Phys. 1981, 74, 4150-4155.
- [52] H. C. Yao, W. G. Rothschild, J. Chem. Phys. 1978, 68, 4774–4780.
- [53] M. Primet, J. Chem. Soc. Faraday Trans. 1 1978, 74, 2570-2580.
- [54] C. A. Rice, S. D. Worley, C. W. Curtis, J. A. Guin, A. R. Tarrer, J. Chem. Phys. J. Chem. Phys. Rh J. Chem. Phys. Rh J. Chem. Phys. 1981, 74(11), 6487–6497, DOI 10.1063/1.440987.
- [55] E. M. James, N. D. Browning, *Ultramicroscopy* **1999**, *78*, 125–139.
- [56] S. Yamashita, J. Kikkawa, K. Yanagisawa, T. Nagai, K. Ishizuka, K. Kimoto, Sci. Rep. 2018, 8, 12325.
- [57] H. F. J. Van't Blik, J. B. A. D. Van Zon, T. Hulzlnga, J. C. Vis, D. C. Koningsberger, R. Prlns, J. Phys. Chem. 1983, 87, 2264–2267.
- [58] F. Solymosi, M. Pásztor, J. Phys. Chem. 1985, 89, 4789–4793.
- [59] F. Solymosi, M. Pásztor, Infrared Study of the Effect of H₂ on CO-Induced Structural Changes in Supported Rh, 1986.
- [60] A. Suzuki, Y. Inada, A. Yamaguchi, T. Chihara, M. Yuasa, M. Nomura, Y. Iwasawa, Angew. Chem. Int. Ed. 2003, 42, 4795–4799; Angew. Chem. 2003, 115, 4943–4947.
- [61] A. Berko, F. Solymosi, J. Catal. 1999, 183, 91–101.
- [62] V. Matolín, M. H. Elyakhloufi, K. Msaek, E. Gillet, Catal. Lett. 1993, 21, 175–182.
- [63] P. Basu, D. Panayotov, J. T. Yates, J. Am. Chem. Soc. 1988, 110, 2074– 2081.
- [64] K. Khivantsev, C. G. Vargas, J. Tian, L. Kovarik, N. R. Jaegers, J. Szanyi, Y. Wang, Angew. Chem. Int. Ed. 2021, 60, 391–398; Angew. Chem. 2021, 133, 395–402.

Manuscript received: October 6, 2022 Revised manuscript received: October 28, 2022